

Electronic Supplementary Information

A New Photoelectrochemical Biosensor based on FeOOH and Exonuclease III-aided Dual Recycling Signal Amplification for HPV-16

Detection

Yanlin Wang, Lingying Xia, Xuelian Xiang, Ruo Yuan* and Shaping Wei*

Key Laboratory of Luminescence Analysis and Molecular Sensing (Southwest University), Ministry of Education, College of Chemistry and Chemical Engineering, Southwest University, Chongqing 400715, PR China

* Corresponding author. Tel: +86-23-68252277, fax: +86-23-68253172.
E-mail address: yuanruo@swu.edu.cn (R. Yuan), shapingw@swu.edu.cn (S. P. Wei).

1. Materials and Regents

Ferric chloride hexahydrate ($\text{FeCl}_3 \cdot 6\text{H}_2\text{O}$, 99.0%) and sodium sulfate (Na_2SO_4) were purchased from Chemical Reagent Co. (Chongqin, China). Bovine serum albumin (BSA), gold chloride tetrahydrate ($\text{HAuCl}_4 \cdot 4\text{H}_2\text{O}$), tris(2-carboxyethyl)-phosphine (TCEP), tetraethylorthosilicate (TEOS), ammonium hydroxide ($\text{NH}_3 \cdot \text{H}_2\text{O}$) (28%) and (3-aminopropyl) triethoxysilane (APTES) were supplied by Sigma Chemical Co. (St. Louis, MO, USA). Hydrogen peroxide (H_2O_2 , 30%) and glutaraldehyde (50%) were provided by Kelong Chemical Inc. (Chengdu, China). $\text{K}_3[\text{Fe}(\text{CN})_6]$ and $\text{K}_4[\text{Fe}(\text{CN})_6]$ were obtained from Beijing Chemical Reagent Co. (Beijing, China). Phosphate buffered solution (PBS, pH 7.4) was prepared by 0.1 M KCl, 0.1 M KH_2PO_4 and 0.1 M Na_2HPO_4 . TBE buffer (5 \times ; 250 mM Tris, 250 mM H_3BO_3 , 10 mM EDTA; pH 8.0) was applied for the polyacrylamide-gel-electrophoresis (PAGE) experiments. All DNA, Exonuclease III (Exo III) and 10 \times NE Buffer were acquired from Sangon Biotech Co. Ltd (Shanghai, China). The human blood serum samples were provided by the Ninth People's Hospital of Chongqing, China. The sequences used in the experiment were listed as the following (Table S1):

Table S1. Sequences used in the experiment

Name	Sequence (5' → 3')
Hairpin DNA1 (HP1)	GGA CTG GAT ACG CAC GAC CTAG TTTT CTA GGT CGT GCG
	TAT CCA GTC CAT CTC TAC TGT TAT GAG
Single-stranded DNA1 (S1)	GGA TAC GCA CGA CTC TAG

Single-stranded DNA2 (S2)	CTA GGT CGT GCG TAT CCA GTC C
Hairpin DNA2 (HP2)	GGA TAC GCG CAG AGT CGT GCG TAT CCA C-SH
Signal probe DNA (SP)	GCG CGT ATC CAG TTT TT-NH ₂
Target (HPV-16)	CTC ATA ACA GTA GAG ATC AGT T
Single-base mismatched DNA (1c)	CTC ATA ACA GAA GAG ATC AGT T
Three-base mismatched DNA (3c)	CTC ATA ACA GAA GTG CTC AGT T
Random DNA (random)	TGC CCA GGT ACA GGA GAC TGT GTA GAA GCA

2. Apparatus

All PEC measurements were performed on a PEC workstation (Ivium, Netherlands) and equipped with a three-electrode system including glassy carbon electrode (GCE, $\Phi = 4$ mm) as the working electrode, a platinum wire as the counter electrode, and an Ag/AgCl as the reference electrode, respectively. A CHI 660E electrochemistry workstation (Shanghai Chenhua Instrument, China) was used to measure the electrochemical impedance spectroscopy (EIS). The characterizations of the prepared materials were tested by scanning electron microscopy (SEM, S-4800, Hitachi, Japan), UV-2450 UV-visible (UV-vis) absorption spectrums (Shimadzu, Tokyo, Japan), X-ray photoelectron spectroscopy (XPS, Thermoelectricity Instruments, U.S.A.). Transmission electron microscopy (TEM) images and energy dispersive spectrum (EDS) mapping images were taken using a FEI Talos F200X microscope operated at 200kv by drop casting the material dispersions on carbon-coated Cu grids and drying under ambient conditions. Powder X-ray diffraction (XRD) patterns

were performed on a XD-3 X-ray diffractometer with Cu K α radiation (Purkinje, China). The Fourier transform infrared (FTIR) spectra were carried out using Spectrum GX FTIR spectroscopy system (PerkinElmer, U.S.A.). Raman spectra were carried out on a Renishaw inVia confocal Raman microscope system (Renishaw, UK).

3. Synthesis of FeOOH

The FeOOH was prepared according to the previous method with minor modification.¹ In brief, FeCl₃·6H₂O (1.0812 g) and Na₂SO₄ (0.5682 g) were mixed in 60 mL ultrapure water and kept stirring for 1 h. Subsequently, the mixture was transferred to a 100 mL Teflon-lined stainless-steel autoclave and kept at 120 °C for 6 h. After cooling to room temperature, the obtained product was collected and cleaned several times with ultrapure water by centrifugation, and finally dried at 60 °C.

4. Preparation of SP-SiO₂ NPs

The synthesis method of amino-modified SiO₂ NPs (SiO₂-NH₂ NPs) was based on the previous literature with minor modification.² The obtained SiO₂-NH₂ NPs were purified by centrifugation with ethanol, and then redispersed in 10 mL PBS solution (pH 7.4). After that, 50 μ L of SiO₂-NH₂ NPs and 100 μ L of glutaraldehyde (0.05%) were mixed with 1 mL of SP (2.5 μ M) and stirred at room temperature for 2 h. Finally, the obtained SP-SiO₂ NPs was centrifugated and redispersed in 1 mL PBS (pH 7.4) solution and stored at 4 °C for further use.

5. Exo III-aided Dual Recycling Signal Amplification

The detailed process of Exo III-aided dual recycling signal amplification was as follows. First, all DNA were diluted in PBS solution (pH 7.4) and stored at 4 °C when not in use. Besides, HP1 was heated to 95 °C for 5 min and cooled to room temperature to form the hairpin DNA before use. Second, S1 (2 μM, 50 μL) and S2 (2 μM, 50 μL) were mixed together and incubated at 37 °C for 2 h to obtain S1-S2 hybrid duplex. Finally, HP1 (2.5 μM, 15 μL), various concentrations of target (10 μL), S1-S2 (2 μM, 15 μL), 5 μL of 10×NE Exo III buffer and Exo III (25 U) were incubated at 37 °C for 2 h. And then the mixed solution was heated at 80 °C for 15 min to deactivate the Exo III. The final obtained solution was stored at 4 °C for PEC measurement.

6. Fabrication of the PEC Biosensor

Firstly, the GCE was prepared according to the literature.³ Subsequently, the FeOOH solution (0.5 mg/mL, 10 μL) was dropped onto the pretreated electrode and then dried at 37 °C. Next, the gold nanoparticles (Au NPs) modified GCE (Dep Au/GCE) was obtained by immersing the modified electrode into 1% HAuCl₄ solution and electrodepositing under -0.2 V for 15 s. Followed by 10 μL of 2 μM HP2 was immobilized on the electrode through the formation of strong Au-S bonds and incubated overnight at 4 °C. After dropping with 10 μL of 1% BSA to eliminate nonspecific binding sites for 40 min, 10 μL of obtained S1 solution was dropped into the modified electrode to hybrid with HP2 for 2 h at 37 °C. Finally, 15 μL SP-SiO₂ NPs was introduced on the electrode for 2 h at 37 °C. The resulting electrode was

employed for the PEC measurements after washing with distilled water.

7. PEC Measurements

The PEC measurement was conducted at 5 mL of PBS solution (0.1 M, pH 7.4) containing 50 μL of H_2O_2 (30%) as the electron donor. The excitation light source (wavelength: $\lambda = 365 \text{ nm}$; radiation flux: $\Phi = 170 \text{ mW}$) was provided by a light-emitting diode (LED) lamp and switched from “off-on-off” for 10 s-20 s-10 s under 0.0 V potential.

8. Other characterizations of FeOOH

Figure S1A-B presented the TEM images of FeOOH, it was observed that the FeOOH was a flower-like shape and composed of nanorods, which agreed well with the SEM images. Meanwhile, the EDS analysis was shown in Figure S1C, and the measured elements peaks demonstrated that the weight percentages (*Wt %*) and atomic percentages (*At %*) of Fe, O were 73.59% and 26.41%, 44.39% and 55.61%, respectively. Besides, from the XRD pattern of the pristine FeOOH (Figure S1D), no diffraction peaks could be detected, revealing an amorphous structure of FeOOH.⁴ Figure S1E presented the FT-IR spectrum of FeOOH, the broad absorption band at 3345 cm^{-1} could be attributed to O-H vibration in FeOOH, while the bands centered at 1424 , 663 and 480 cm^{-1} could be all identified to the Fe-O vibrational modes in FeOOH.^{5,6} The absorption bands at 885 and 793 cm^{-1} were assigned to flexural vibration of Fe-O-H and the peak around 1631 cm^{-1} was related to the adsorption of water molecules on the surface of FeOOH.⁷ The Raman spectrum was shown in

Figure S1F, the characteristic Raman peaks of FeOOH could be observed at 243, 298, 399, 476, 552, 710, 996, and 1254 cm^{-1} , consistent basically with the reported literature.⁵

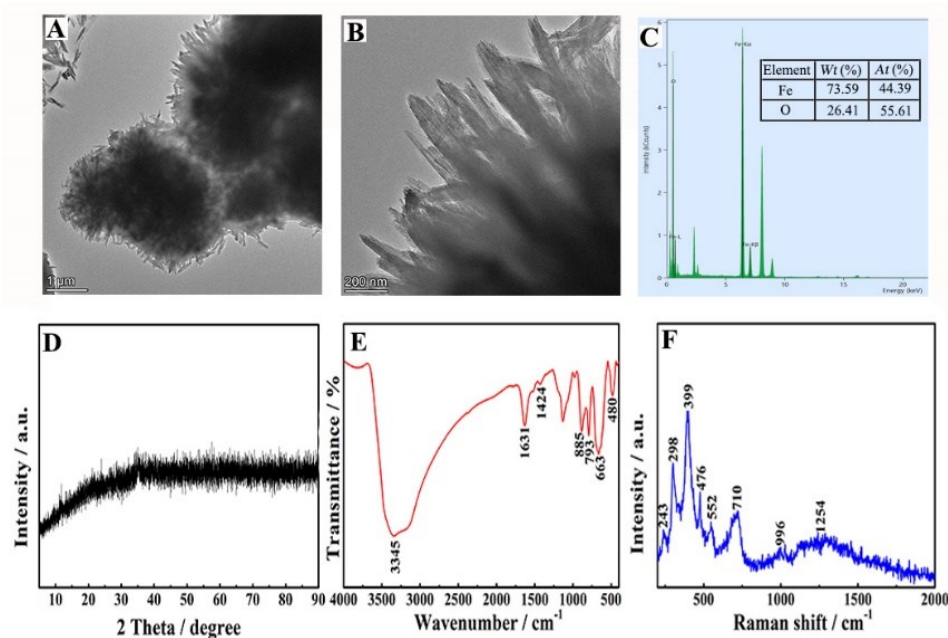


Figure S1: (A) and (B) TEM images of FeOOH; (C) the corresponding EDS analysis spectrogram; (D) XRD analysis of FeOOH; (E) FT-IR spectrum of FeOOH and (F) Raman study of FeOOH.

9. PAGE Characterization of Exo III-aided Dual Recycling Signal Amplification Process

In order to verify the feasibility of the biosensor, 16% PAGE was used to investigate the Exo III-aided dual recycling signal amplification process, and the results were illustrated in Figure S2. Lane 1 and lane 2 represented the HP1 and target, respectively. After target was incubated with HP1, a new bright band with low mobility (HP1-Target hybrid duplex) was obviously appeared (lane 3), indicating that the successful combination of target and HP1. Whereas the bright band was

disappeared with the addition of Exo III and a new and weak band (S0) with a faster mobility was noticed (lane 4), suggesting that the successful digestion of HP1-target hybrid duplex by Exo III. Lane 5 and lane 6 displayed the images of S1 and S2, respectively. After S1 was mixed with S2, a bright band for the hybrid duplex of S1-S2 was observed (lane 7). Upon addition of S0 into lane 7 based system, a new band with lower mobility (top) and a new band with higher mobility (bottom) were appeared (lane 8), suggesting that the S0 could hybrid with S2, leading to form S0-S2 hybrid duplex and release S1 from S1-S2 hybrid duplex. When Exo III was added to the above mixture, it was observed that only a weak band with fast mobility was appeared (lane 9), demonstrating the successful release of S1 from the Exo III-aided dual recycling signal amplification. The PAGE provided effect support of the proposed strategy.

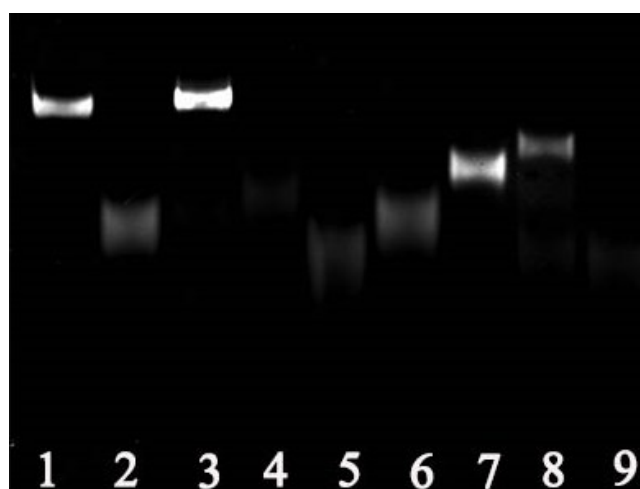


Figure S2. PAGE analysis of the Exo III-aided dual recycling signal amplification process: lane 1, HP1; lane 2, target; lane 3, HP1-Target hybrid duplex; lane 4, S0; lane 5, S1; lane 6, S2; lane 7, S1-S2 hybrid duplex; lane 8, S0 and S1-S2 hybrid duplex; lane 9, S0 and S1-S2 hybrid duplex

incubated with Exo III.

10. Optimization of Experimental Conditions

To acquire a satisfying analytical performance of this biosensor, some parameters including FeOOH concentration, HP1 concentration and Exo III concentration were optimized *via* PEC measurements. As shown in Figure S3A, the initial PEC signal enhanced visibly along with the concentration of FeOOH increased from 0.1 mg/mL to 0.5 mg/mL, while it decreased gradually when the concentration of FeOOH surpassed 0.5 mg/mL, which could be ascribed to the extensive modification of FeOOH on the GCE, resulting in its instability and easy to fall off from the electrode surface. Thus, 0.5 mg/mL was selected as the optimal concentration of FeOOH. Besides, as depicted in Figure S3B, the PEC signal decreased with the increasing concentration of HP1 until a plateau was reached 2.5 μ M. Thus, the HP1 concentration of 2.5 μ M was used for the subsequent experiments. Moreover, as shown in Figure S3C, for Exo III concentration, the PEC signal decreased with the increasing concentration of Exo III and reached equilibrium when the concentration was 25 U. Consequently, 25 U of Exo III concentration was selected for further experiments.

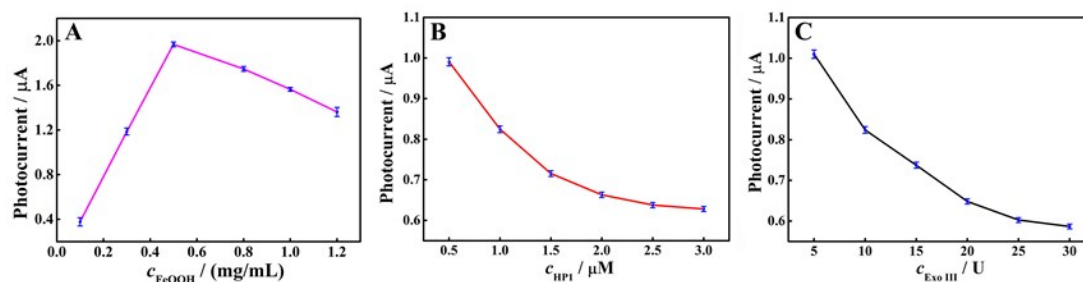


Figure S3. The conditions optimization of (A) the concentration of FeOOH, (B) the concentration

of HP1 and (C) the concentration of Exo III.

11. SEM characterizations of the electrode surface

The scanning electron microscope (SEM) was employed to characterize the comparison of the electrode surface before and after the detection. The conductive glass (CG) was used as a substrate to immobilize materials for analyzing. Figure S5A and S5B presented different SEM resolutions in the absence of target. As illustrated in Figure S5C and S5D, a rough surface covered the modified CG surface could be observed in the presence of target, which could be attributed to that the large amounts of SiO₂ were widely dispersed on the CG surface. The above characterization results exhibited distinct changes of the electrode surface before and after the detection.

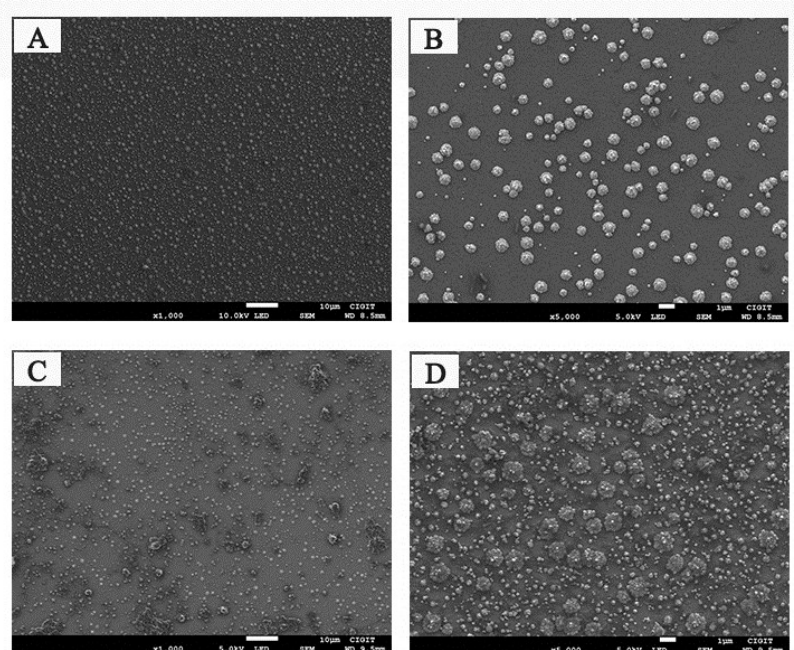


Figure S5. SEM images of (A-B) in the absence of target and (C-D) in the presence of target under different resolutions.

12. Recovery Test of HPV-16 in Serum

In order to explore the feasibility of the constructed PEC biosensing platform,

different concentrations of target (from 0.01 pM to 10 pM) were diluted in human serum samples (50-fold diluted by PBS, pH 7.4). As shown in Table S2, the recovery ranged from 93.3 to 101.7% with RSD varied between 0.97 and 1.99%, suggesting a potential application for HPV-16 detection in complex biological systems.

Table S2. Recovery assay for HPV-16 in human serum samples.

Sample	Added/pM	Found/pM	Recovery/%	RSD/%
1	0.01	0.00933	93.3	1.26
2	0.1	0.09938	99.4	0.97
3	1	1.017	101.7	1.79
4	10	9.872	98.7	1.99

Table S3. Comparison of this PEC sensor with other sensors for HPV-16 detection.

Analytical method	Linear range	Detection limit	Ref.
Fluorescence	5 nM to 1 μ M	1.23 nM	8
LFSB	5 nM to 100 nM	1.0 nM	9
ECL	0.1 nM to 200 nM	0.03 nM	10
SWV	500 pM to 100 nM	200 pM	11
Colorimetry	10 pM to 1 μ M	10 pM	12
EIS	1 pM to 1 μ M	150 fM	13
DPV	100 fM to 10 nM	40.3 fM	14
PEC	0.5 fM to 1 nM	0.17 fM	<i>This work</i>

Abbreviations: lateral flow strip biosensor (LFSB); electrochemiluminescence (ECL); square wave voltammetry (SWV); electrochemical impedance spectroscopy (EIS); differential pulse

voltammetry (DPV).

Table S4. A summary of recently developed other viruses based on PEC model.

Target	Materials used	Linear range	Detection limit	Ref.
NoV	CdS QDs	2×10^{-4} to 2×10^{-10} g/mL	2×10^{-10} g/mL	15
HTLV-I	RGO/CdS QDs/ZnS	50 aM to 100 pM	11.3 aM	16
ALVs-J	W-Bi ₂ S ₃ /PTBA	$10^{2.08}$ to $10^{4.02}$ TCID ₅₀ /mL	97 TCID ₅₀ /mL	17
HBsAg	GNPs/ZnAgInS QDs	0.005 to 30 ng/mL	0.5 pg/mL	18
HIV	β -CD/CdS NRs	10 fM to 1 nM	1.16 fM	19

Abbreviations: norovirus (NoV); human T-cell lymphotropic virus type I (HTLV-I); subgroup J of avian leukosis virus (ALVs-J); hepatitis B virus surface antigen (HBsAg); human immune deficiency virus (HIV).

References

1. S. Agarwala, Z. H. Lim, E. Nicholsonb and G. W. Ho, *Nanoscale*, 2012, **4**, 194-205.
2. H. H. Wang, M. J. Li, Y. N. Zheng, T. Hu, Y. Q. Chai and R. Yuan, *Biosens. Bioelectron.*, 2018, **120**, 71-76.
3. H. M. Deng, Y. Q. Chai, R. Yuan and Y. L. Yuan, *Anal. Chem.*, 2020, **92**, 8364-8370.
4. J. Q. Liu, M. B. Zheng, X. Q. Shi, H. B. Zeng, H. Xia, *Adv. Funct. Mater.*, 2016, **26**, 919-93.
5. Y. J. Ai, L. Liu, C. Zhang, L. Qi, M. Q. He, Z. Liang, H. B. Sun, G. A. Luo and Q. L. Liang, *ACS Appl. Mater. Interfaces.*, 2018, **10**, 32180-32191.
6. A. Malathi, Prabhakarn Arunachalam, J. Madhavan, A. M. Al-Mayouf and M. Ghanem, *Colloids and Surfaces A*, 2018, **537**, 435-445.
7. Y. W. Li, L. Liu, J. H. Feng, X. Ren, Y. Zhang, T. Yan, X. J. Liu, Q. Wei, *Biosens. Bioelectron.*, 2020,

- 154**, 112089.
8. L. H. Chen, M. C. Liu, Y. Tang, C. F. Chen, X. X. Wang and Z. Q. Hu, *ACS Appl. Mater. Interfaces*, 2019, **11**, 18637-18644.
 9. Z. Yang, C. Yi, S. J. Lv, Y. H. Sheng, W. Wen, X. H. Zhang and S. F. Wang, *Sens. Actuators, B.*, 2019, **285**, 326-332.
 10. Y. X. Nie, X. Zhang, Q. Zhang, Z. H. Liang, Q. Ma and X. G. Su, *Biosens. Bioelectron.*, 2020, **160**, 112217.
 11. A. Jimenez Jimenez, B. Ruttkay-Nedecky, S. Dostalova, L. Krejcova, P. Michalek, L. Richtera and V. Adam, *Int. J. Mol. Sci.*, 2016, **17**, 585.
 12. S. Persano, P. Valentini, J. H. Kim and P. P. Pompa, *Chem. Commun.*, 2013, **49**, 10605-10607.
 13. A. Karimizefreh, F. A. Mahyari, M. VaezJalali, R. Mohammadpour and P. Sasanpour, *Microchim Acta.*, 2017, **184**, 1729-1737.
 14. H. Y. Huang, W. Q. Bai, C. X. Dong, R. Guo and Z. H. Liu, *Biosens. Bioelectron.*, 2015, **68**, 442-446.
 15. J. B. Guo, D. Liu, Z. Q. Yang, W. C. Weng, E. W. C. Chan, Z. L. Zeng, K.Y. Wong, P. Lin and S. Chen, *Bioelectrochemistry*, 2020, **136**, 107591.
 16. X. M. Shi, G. C. Fan, X. Y. Tang, Q. M. Shen and J. J. Zhu, *Biosens. Bioelectron.*, 2018, **109**, 190-196.
 17. B. Sun, J. Dong, W. J. Shi and S. Y. Ai, *Sens. Actuators, B.*, 2016, **229**, 75-81.
 18. Y. Hu, Y. J. Huang, Y. Y. Wang, C. Y. Li, W. L. Wong, X. X. Ye and D. Sun, *Analytica Chimica Acta*, 2018, **1035**, 136-145.
 19. J. Fan, Y. Zang, J. J. Jiang, J. P. Lei, H. G. Xue, *Biosens. Bioelectron.*, 2019, **142**, 111557.